Proceedings of the Ninth International Conference on Applications of Statistics and Probability in Civil Engineering (ICASP9), San Francisco, USA, July 6-9, 2003

Convergence Studies in Nonlinear Finite Element Response Sensitivity Analysis

Quan Gu & Joel P. Conte
Department of Structural Engineering, University of California at San Diego, La Jolla, CA, USA

Keywords: Earthquake engineering, finite element analysis, sensitivity analysis, convergence studies

ABSTRACT: A method to compute the "exact" or consistent sensitivities to material and loading parameters of the numerical nonlinear finite element response was developed by other researchers and the second author. This general method is referred to in the literature as the Direct Differentiation Method (DDM). This paper focuses on the behavior of stand-alone sensitivity results. It presents the results of convergence studies of the DDM performed in the context of materially-nonlinear-only finite element models of frame structures and for two types of analysis commonly used in earthquake engineering, namely nonlinear static push-over analysis and nonlinear response history analysis. Convergence of nonlinear finite element response sensitivities obtained using forward finite difference analysis towards those obtained using the DDM is examined. Convergence of response sensitivities with progressive refinement of both the spatial and temporal discretizations is also investigated based on some application examples. Convergence of response sensitivities is compared with convergence of the corresponding response parameters. Both global (e.g., floor displacement) and local (i.e., plastic curvature, accumulated plastic curvature) response parameters are considered.

1 INTRODUCTION

In the last decade, finite element reliability methods (FERM's) have emerged as a powerful tool to perform probabilistic performance assessment of large and complex structural systems (Liu and Der Kiureghian 1991, Li and Der Kiureghian 1995, Conte et al. 1995, 1998, 2000). They allow the use of the same state-of-the-art computational nonlinear structural models as those used in deterministic response analysis of these systems. Accurate and efficient computation of the gradient or sensitivities to material and loading parameters of structural response parameters used in formulating the various limit-state functions are important requirements and ingredients of FERM's. Finite element response sensitivity analysis also plays an important role in structural optimization and system identification based on (linear or nonlinear) finite element model updating.

An algorithm for computing the "exact" or consistent sensitivities of the computationally simulated structural response to constitutive material parameters and discrete loading parameters consists of differentiating exactly (consistently) the finite element numerical scheme (including the material constitutive law integration scheme) with respect to the sensitivity parameters. This algorithm and its implementation in a general-purpose nonlinear finite element analysis program have been described in the literature (Zhang and Der Kiureghian 1993, Conte et al. 2001, 2002). This method is referred to here as the Direct Differentiation Method (DDM).

This paper focuses entirely on the behavior of stand-alone sensitivity analysis. It appears that this type of study is not found in many other places in the literature. More specifically, this paper presents the results of the following convergence studies performed on the DDM as applied to an inelastic frame structure: (1) convergence of response sensitivities obtained using forward finite difference analysis towards those obtained using the DDM; (2) convergence of DDM results with respect to the spatial discretization (i.e., finite element mesh size); and (3) convergence of DDM results with respect to the temporal discretization (i.e., time step size). This paper also compares (1) the convergence rate of various response parameters with that of their respective sensitivities, (2) the convergence rate of global and local response parameters, (3) the convergence rate of global and local response sensitivities.

2 "EXACT" FINITE ELEMENT RESPONSE SENSITIVITY ANALYSIS

After spatial discretization using the finite element method, the equation of motion of a materially-non-linear-only structural system is given by the following nonlinear matrix differential equation:

$$\boldsymbol{M}(\theta)\ddot{\boldsymbol{u}}(t,\theta)+\boldsymbol{C}(\theta)\dot{\boldsymbol{u}}(t,\theta)+\boldsymbol{R}(\boldsymbol{u}(t,\theta),\theta)=\boldsymbol{F}(t,\theta) \quad (1)$$

where t = time, θ = scalar sensitivity parameter (material or loading variable), $\boldsymbol{u}(t)$ = vector of nodal displacements, $\boldsymbol{C}$ = damping matrix, $\boldsymbol{M}$ = mass matrix, $\boldsymbol{R}(\boldsymbol{u},t)$ = history dependent internal (inelastic) resisting force vector, $\boldsymbol{F}(t)$ = dynamic load vector, and a superposed dot denotes one differentiation with respect to time. The potential dependence of each term of the equation of motion on the sensitivity parameter θ is shown explicitly in Eq. (1).

We assume that the equation of motion (1) is integrated numerically in time using the well-known Newmark-β method of structural dynamics (Chopra 2001), i.e.,

$$\begin{aligned}\ddot{\boldsymbol{u}}_{n+1}&=\left(1-\frac{1}{2\beta}\right)\ddot{\boldsymbol{u}}_n-\frac{1}{\beta(\Delta t)}\dot{\boldsymbol{u}}_n+\frac{1}{\beta(\Delta t)^2}(\boldsymbol{u}_{n+1}-\boldsymbol{u}_n)\\ \dot{\boldsymbol{u}}_{n+1}&=(\Delta t)\left(1-\frac{\alpha}{2\beta}\right)\ddot{\boldsymbol{u}}_n+\left(1-\frac{\alpha}{\beta}\right)\dot{\boldsymbol{u}}_n\\ &\quad+\frac{\alpha}{\beta(\Delta t)}(\boldsymbol{u}_{n+1}-\boldsymbol{u}_n)\end{aligned} \quad (2)$$

where we select $\alpha = 1/2$, $\beta = 1/4$ for the constant average acceleration method. Substitution of Eqs. (2) into equation of motion (1) expressed at discrete time $t = t_{n+1} = (n+1)\,\Delta t$, in which Δt denotes the constant time increment, yields the following nonlinear matrix algebraic equation in the unknowns $\boldsymbol{u}_{n+1} = \boldsymbol{u}(t_{n+1})$:

$$\begin{aligned}\boldsymbol{\Psi}(\boldsymbol{u}_{n+1}) &= \tilde{\boldsymbol{F}}_{n+1}-\left[\frac{1}{\beta(\Delta t)^2}\boldsymbol{M}\boldsymbol{u}_{n+1}\right.\\ &\quad\left.+\frac{\alpha}{\beta(\Delta t)}\boldsymbol{C}\boldsymbol{u}_{n+1}+\boldsymbol{R}(\boldsymbol{u}_{n+1})\right] = \boldsymbol{0}\end{aligned} \quad (3)$$

where

$$\begin{aligned}\tilde{\boldsymbol{F}}_{n+1} &= \boldsymbol{F}_{n+1}+\boldsymbol{M}\left[\frac{1}{\beta(\Delta t)^2}\boldsymbol{u}_n+\frac{1}{\beta(\Delta t)}\dot{\boldsymbol{u}}_n-\left(1-\frac{1}{2\beta}\right)\ddot{\boldsymbol{u}}_n\right]\\ &\quad+\boldsymbol{C}\left[\frac{\alpha}{\beta(\Delta t)}\boldsymbol{u}_n-\left(1-\frac{\alpha}{\beta}\right)\dot{\boldsymbol{u}}_n-(\Delta t)\left(1-\frac{\alpha}{2\beta}\right)\ddot{\boldsymbol{u}}_n\right]\end{aligned}$$

Equation (3) is solved using a Newton-Raphson iterative procedure (Simo and Hughes 1998). Assuming that $\boldsymbol{u}_{n+1}$ is the converged solution for the current time step, and differentiating Eq. (3) with respect to θ using the chain rule, recognizing that $\boldsymbol{\sigma} = \boldsymbol{\sigma}(\boldsymbol{\epsilon}(t,\theta),\theta)$ where $\boldsymbol{\sigma}$ and $\boldsymbol{\epsilon}$ denote the stress and strain tensors, respectively, we obtain:

$$\begin{aligned}&\left[\frac{1}{\beta(\Delta t)^2}\boldsymbol{M}+\frac{\alpha}{\beta(\Delta t)}\boldsymbol{C}+(\boldsymbol{K}_T^{stat})_{n+1}\right]\frac{\partial\boldsymbol{u}_{n+1}}{\partial\theta} =\\ &\quad-\left(\frac{1}{\beta(\Delta t)^2}\frac{\partial\boldsymbol{M}}{\partial\theta}+\frac{\alpha}{\beta(\Delta t)}\frac{\partial\boldsymbol{C}}{\partial\theta}\right)\boldsymbol{u}_{n+1}\\ &\quad-\left.\frac{\partial\boldsymbol{R}(\boldsymbol{u}_{n+1}(\theta),\theta)}{\partial\theta}\right|_{\boldsymbol{u}_{n+1}}+\frac{\partial\tilde{\boldsymbol{F}}_{n+1}}{\partial\theta}\end{aligned} \quad (4)$$

where

$$\begin{aligned}\frac{\partial\tilde{\boldsymbol{F}}_{n+1}}{\partial\theta} &= \frac{\partial\boldsymbol{F}_{n+1}}{\partial\theta}+\\ &\frac{\partial\boldsymbol{M}}{\partial\theta}\left(\frac{1}{\beta(\Delta t)^2}\boldsymbol{u}_n+\frac{1}{\beta(\Delta t)}\dot{\boldsymbol{u}}_n-\left(1-\frac{1}{2\beta}\right)\ddot{\boldsymbol{u}}_n\right)+\\ &\boldsymbol{M}\left[\frac{1}{\beta(\Delta t)^2}\frac{\partial\boldsymbol{u}_n}{\partial\theta}+\frac{1}{\beta(\Delta t)}\frac{\partial\dot{\boldsymbol{u}}_n}{\partial\theta}-\left(1-\frac{1}{2\beta}\right)\frac{\partial\ddot{\boldsymbol{u}}_n}{\partial\theta}\right]+\\ &\frac{\partial\boldsymbol{C}}{\partial\theta}\left[\frac{\alpha}{\beta(\Delta t)}\boldsymbol{u}_n-\left(1-\frac{\alpha}{\beta}\right)\dot{\boldsymbol{u}}_n-(\Delta t)\left(1-\frac{\alpha}{2\beta}\right)\ddot{\boldsymbol{u}}_n\right]+\\ &\boldsymbol{C}\left[\frac{\alpha}{\beta(\Delta t)}\frac{\partial\boldsymbol{u}_n}{\partial\theta}-\left(1-\frac{\alpha}{\beta}\right)\frac{\partial\dot{\boldsymbol{u}}_n}{\partial\theta}-(\Delta t)\left(1-\frac{\alpha}{2\beta}\right)\frac{\partial\ddot{\boldsymbol{u}}_n}{\partial\theta}\right]\end{aligned}$$

The second term on the right-hand-side of Eq. (4) represents the partial derivative of the internal resisting force vector, $\boldsymbol{R}(\boldsymbol{u}_{n+1})$, with respect to sensitivity parameter θ under the condition that the displacement vector $\boldsymbol{u}_{n+1}$ remains fixed. In displacement-based finite element analysis, this conditional derivative term can be expressed as (Conte et al. 2002)

$$\begin{aligned}&\left.\frac{\partial\boldsymbol{R}(\boldsymbol{u}_{n+1}(\theta),\theta)}{\partial\theta}\right|_{\boldsymbol{u}_{n+1}} =\\ &\mathop{\mathbf{A}}_{e=1}^{Nel}\int_{\Omega_e}\boldsymbol{B}^T(\boldsymbol{x})\cdot\left.\frac{\partial\boldsymbol{\sigma}(\boldsymbol{x})}{\partial\theta}\right|_{\boldsymbol{\epsilon}_{n+1}(\boldsymbol{x})}\cdot d\Omega_e\end{aligned} \quad (5)$$

where $\left.\frac{\partial\boldsymbol{\sigma}(\boldsymbol{x})}{\partial\theta}\right|_{\boldsymbol{\epsilon}_{n+1}(\boldsymbol{x})}$ denotes the derivative of the stress vector $\boldsymbol{\sigma}(\boldsymbol{\epsilon}_{n+1}(\theta),\theta)$ with respect to θ for fixed strain vector $\boldsymbol{\epsilon}_{n+1}$.

Analytical expressions for this history dependent conditional derivative of the stress vector have been derived by Zhang and Der Kiureghian (1993) and Conte and co-workers (1995a, 1998) for the constitutive J_2 (or Von Mises) plasticity model and by Conte and co-workers (1995a, 1995b) for the constitutive cap plasticity model in the case of a return map constitutive integration algorithm (Simo and Hughes 1998). The above DDM for displacement-based finite elements has been implemented in the general-purpose finite element analysis program FEAP (Taylor 1998).

3 CONVERGENCE STUDIES

This section presents results of convergence studies performed on the DDM as applied to an inelastic test structure.

3.1 Application examples

The test structure considered in this study consists of a five-story single-bay steel moment-resisting frame, a finite element model of which is shown in Fig. 1.

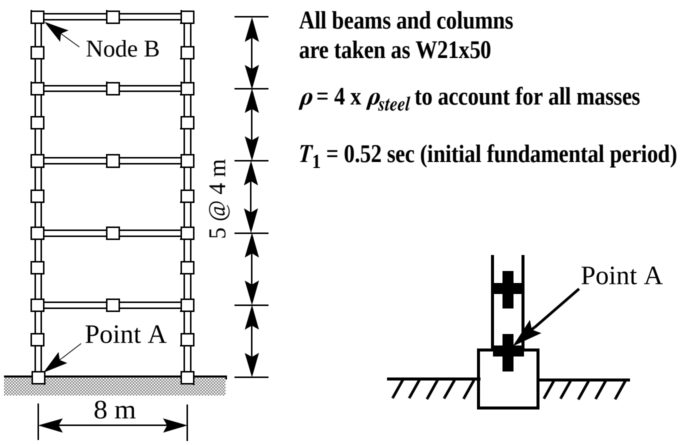

Figure 1. Finite Element model of test structure.

This frame is subjected to (a) a nonlinear static push-over analysis under an inverted triangular pattern of horizontal loads applied at floor levels as shown in Fig. 2, and (b) a nonlinear response history analysis for earthquake base excitation. This frame is modeled using a displacement-based simplified distributed plasticity 2-D beam-column element implemented in FEAP (Taylor 1998). Unless mentioned otherwise, the frame is modeled using two and three elements per beam/column in the static and dynamic case, respectively (Fig. 2). The source of material nonlinearity is the moment-curvature rela-

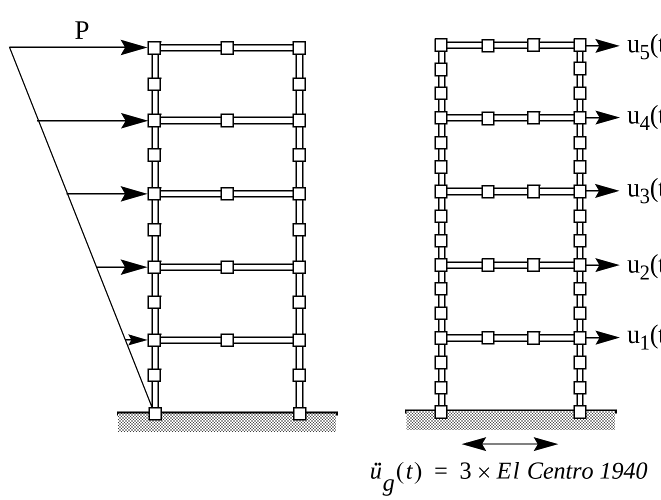

Figure 2. Load cases: static push-over and earthquake base excitation.

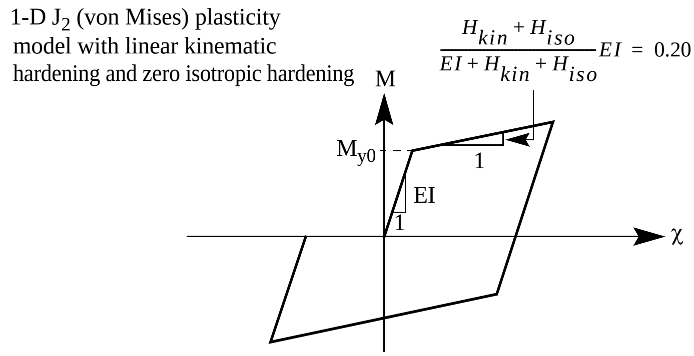

Figure 3. Section constitutive model (moment-curvature).

tion, which is modeled using the 1-D J_2 plasticity model with linear kinematic hardening and zero isotropic hardening as shown in Fig. 3. The axial force - axial strain relation is taken as linear elastic and uncoupled from the flexural behavior. The effects of shear deformations are neglected. All columns and beams of the frame are $W21 \times 50$ steel I-beams with a yield moment $M_{y0} = 384.2 \ [kN \cdot m]$. A 20 percent post-yield to initial flexural stiffness ratio is assumed. A material density of 4 times the mass density of steel, i.e., $\rho = 31,600 \ [kg \cdot m^{-3}]$, is used to account for typical additional masses (e.g., slabs, cross-beams, floors, ceilings, ...). The frame has an initial fundamental period of 0.52 sec. Young's modulus of steel is taken as $E = 2 \times 10^8 \ [kPa]$. The isotropic and kinematic hardening moduli are $H_{iso} = 0$ and $H_{kin} = 20,480 \ [kN \cdot m^2]$, respectively. The cross-sectional properties of the beams/columns are $A = 9.484 \times 10^{-3} \ [m^2]$ and $I = 4.096 \times 10^{-4} \ [m^4]$. There are 5 Gauss-Lobato points per beam-column element. For the static push-over, the lateral force P applied at the roof level (Fig. 2) increases from 0 to 230.5 [*kN*]. In the dynamic case, no damping is included in the model and the earthquake input is taken as the balanced 1940 El Centro record (Fig. 4) scaled by a factor 3. During both the static push-over and the dynamic response, the frame yields significantly.

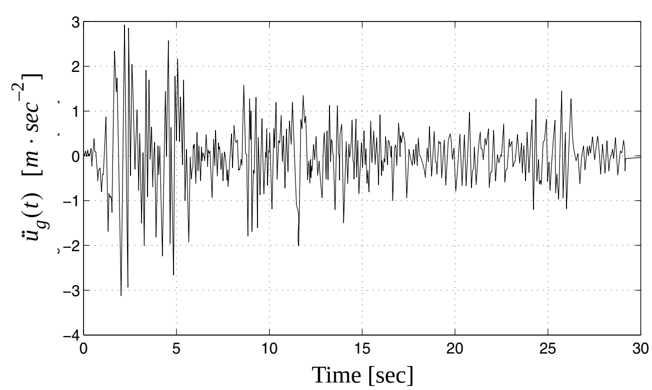

Figure 4. 1940 El centro earthquake record (N-S comp.).

The following five sensitivity parameters are considered in the response sensitivity studies presented below: moment of inertia, I, of cross-section of beams/columns, initial yield moment, M_{y0}, isotropic and kinematic hardening moduli, H_{iso} and H_{kin}, earthquake ground acceleration at time t = 4.22 sec and t = 7.60 sec, $\ddot{u}_g(t = 4.22\ sec)$ and $\ddot{u}_g(t = 7.60\ sec)$.

3.2 Convergence of Finite Difference Calculations of Response Sensitivities towards DDM Results

Here we study the sensitivities of the horizontal displacement response of Node B (Fig. 1) as the frame is subjected to the monotonic static push-over and the ground excitation separately. A set of different relative sensitivity parameter increments, $\Delta\theta/\theta$, is used to study the convergence of response sensitivity results obtained using forward finite difference analysis to those obtained using the DDM. Finite difference and DDM results expressed in normalized or semi-normalized forms are compared in Figs. 5 and 6 for the static push-over analysis with sensitivity parameters I and H_{kin}, and in Figs. 7 and 8 for the dynamic case with sensitivity parameters I and $\ddot{u}_g(t = 4.22\ sec)$. It is observed that for each loading case and for each sensitivity parameter θ, there is an optimum value of $\Delta\theta/\theta$ that makes the finite difference result closest to the DDM result. When the relative sensitivity parameter increment grows above this optimum value, the finite difference results worsens due to truncation error (i.e., effects of higher order terms in Taylor series expansion of response parameter). If we decrease the relative sensitivity parameter increment below this optimum value, so as to reduce the truncation error, we have an excessive condition error. The latter is due to round-off errors in the computer or occurs if the response is calculated by an iterative process which is terminated early (as is the case for the incremental-iterative Newton-Raphson method). In some cases, there may not be any sensitivity parameter increment $\Delta\theta$ which yields an acceptable error. This is the so-called "step-size dilemma." It is noteworthy that for a given structural system, the optimum value of $\Delta\theta/\theta$ depends on the parameter θ and the load case. For the response analyses considered here, the optimum value and acceptable range of the sensitivity parameters are summarized in Table 1. Notice that in Table 1, ΔH_{iso} is not normalized because the nominal value of H_{iso} is zero (i.e., no isotropic hardening). It is observed that in the dynamic case, the optimum value of $\Delta\theta/\theta$ is at least one order of magnitude larger for the discrete loading sensitivity parameter than for the material sensitivity parameters.

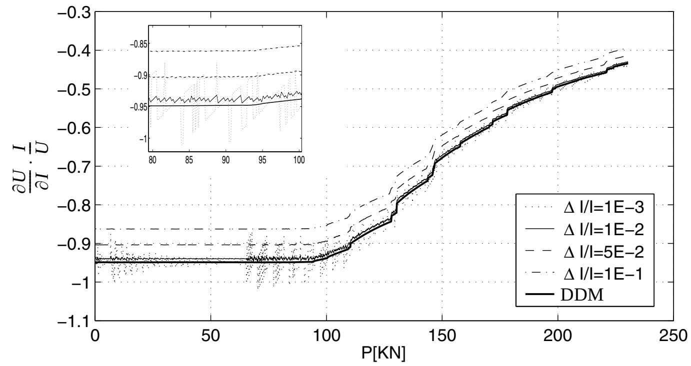

Figure 5. Sensitivity of roof displacement to I.

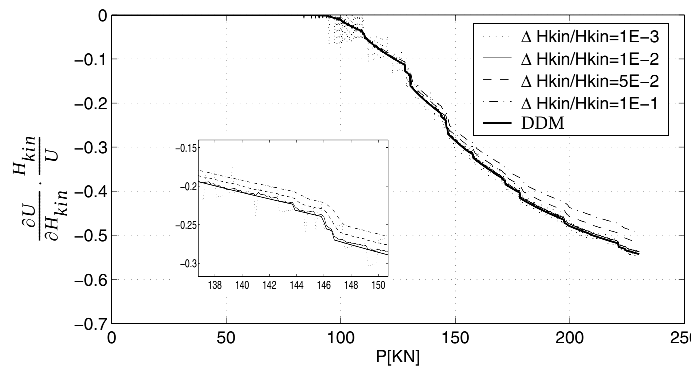

Figure 6. Sensitivity of roof displacement to H_{kin}.

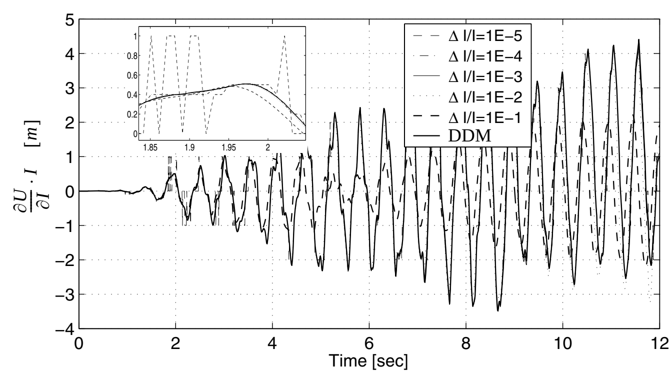

Figure 7. Sensitivity of roof displacement to I.

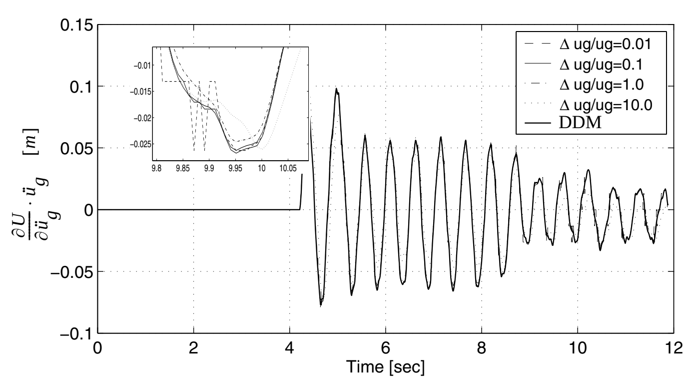

Figure 8. Sensitivity of roof displacement to $\ddot{u}_g(t = 4.22\ sec)$.

Table 1: Optimum values and acceptable ranges for $\Delta\theta/\theta$.

		Material sensitivity parameters				Earthquake input
	$\frac{\Delta\theta}{\theta}$	$\frac{\Delta I}{I}$	$\frac{\Delta M_{y0}}{M_{y0}}$	$\frac{\Delta H_{kin}}{H_{kin}}$	ΔH_{iso}	$\frac{\Delta \ddot{u}_g}{\ddot{u}_g(4.22\ sec)}$
Static Push-over	Best value	10^{-2}	10^{-2}	10^{-2}	10^{5}	
	Lower range	10^{-3}	10^{-3}	10^{-3}	10^{4}	
	Upper range	10^{-1}	10^{-1}	10^{-1}	10^{6}	
Dynamic case	Best value	10^{-3}	10^{-2}	10^{-2}	10^{4}	10^{-1}
	Lower range	10^{-5}	10^{-4}	10^{-3}	10^{3}	10^{-2}
	Upper range	10^{-1}	1	1	10^{7}	10

3.3 Convergence of response and response sensitivities with respect to spatial discretization

This section examines the convergence of global and local response parameters, as well as their sensitivities, with respect to the spatial discretization (i.e., number of finite elements per beam/column). Here, a global response parameter is taken as the horizontal displacement at node B (Fig. 1), U (i.e., roof displacement), while the local response parameters are chosen as the moment-curvature, $M-\chi$, plastic curvature, χ_p, and accumulated plastic curvature, $\bar{\chi}_p$, at Gauss-Lobato point A at the bottom of the left column of the frame (Fig. 1). The spatial discretization was varied from 1 to 8 finite elements per beam/column. Some computational results are shown in Figs. 9 to 12 for the static push-over case, and in Figs. 13 to 17 for the dynamic case. Furthermore, for each response parameter and load case, the minimum number of elements per beam/column required to achieve convergence of response and response sensitivities is reported in Table 2 for the global response parameter U and in Table 3 for local response parameters $M-\chi$, χ_p and $\bar{\chi}_p$.

From the results obtained, we observe that:

(1) Global response parameters converge with fewer finite elements per beam/column than local response parameters (compare results in Tables 2 and 3).

(2) A given response parameter, global or local, converges with fewer elements per beam/column than its sensitivities. This is due to the fact that the response sensitivities are less smooth than the responses themselves; in fact, the response sensitivities are only piecewise continuous, with discontinuities due to material state transitions between elastic and plastic states at Gauss points (Conte et al. 2002).

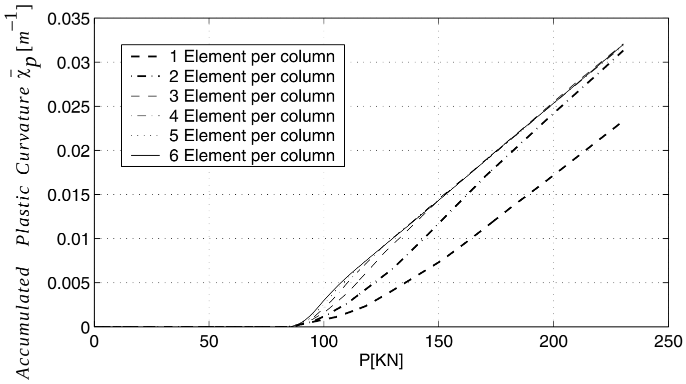

Figure 9. Response parameter $\bar{\chi}_p$ with increasing number of finite elements per beam/column.

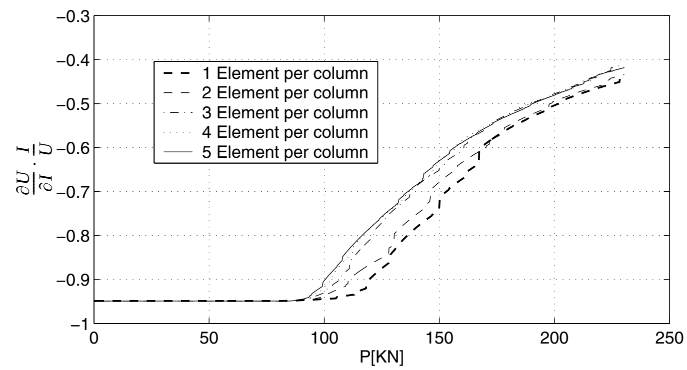

Figure 10. Sensitivity of roof displ. to I with increasing number of finite elements per beam/column.

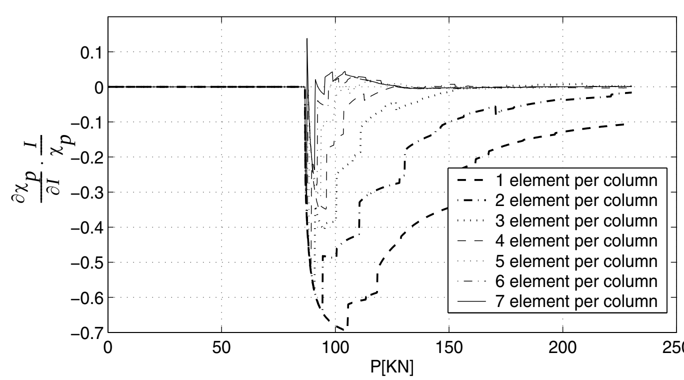

Figure 11. Sensitivity of χ_p to I with increasing number of finite elements per beam/column.

(3) Sensitivities of global response parameters converge with slightly fewer elements per beam/column than sensitivities of local response parameters in the static push-over case. However, this is not always true in the dynamic case.

3.4 Convergence of response and response sensitivities with respect to temporal discretization

In this section, we investigate for the dynamic case the convergence of global and local response parameters, as well as their sensitivities, with respect to the time step size. The frame structure is discretized into

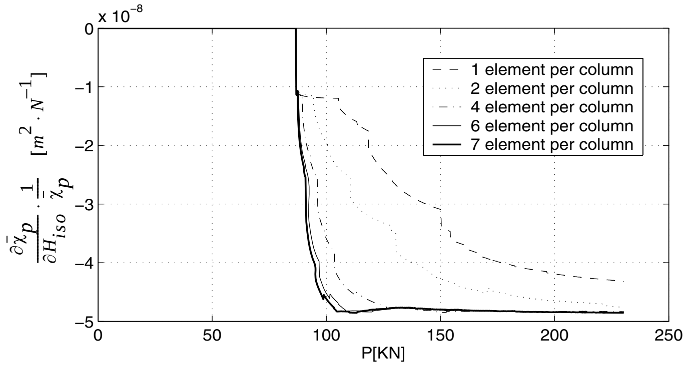

Figure 12. Sensitivity of $\bar{\chi}_p$ to H_{iso} with increasing number of finite elements per beam/column.

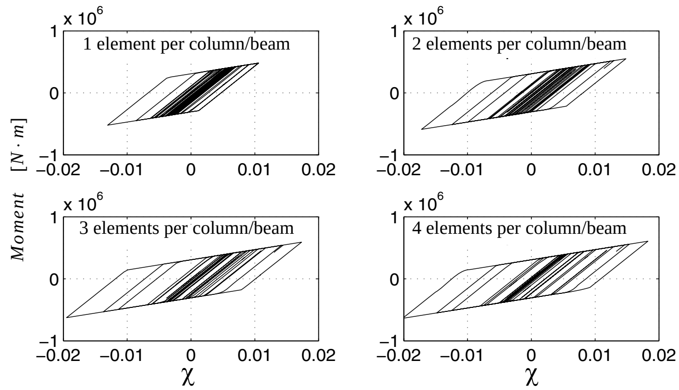

Figure 13. Convergence of moment-curvature response with increasing number of elements per beam/column.

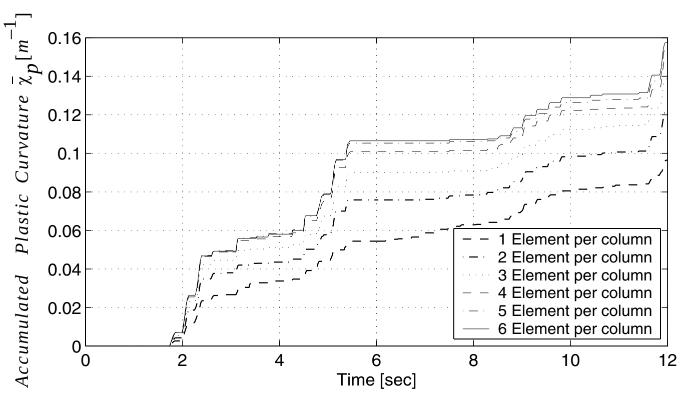

Figure 14. Response parameter $\bar{\chi}_p$ with increasing number of finite elements per beam/column.

Table 2: Minimum number of elements per beam/ column required for convergence of global response and its sensitivities.

	$\frac{\partial U}{\partial I}$	$\frac{\partial U}{\partial M_{y0}}$	$\frac{\partial U}{\partial H_{iso}}$	$\frac{\partial U}{\partial H_{kin}}$	$\frac{\partial U}{\partial \ddot{u}_g(7.60 sec)}$	U
Static Push-over	4	5	4	4		3
Dynamic case	6	9	9	7	7	3

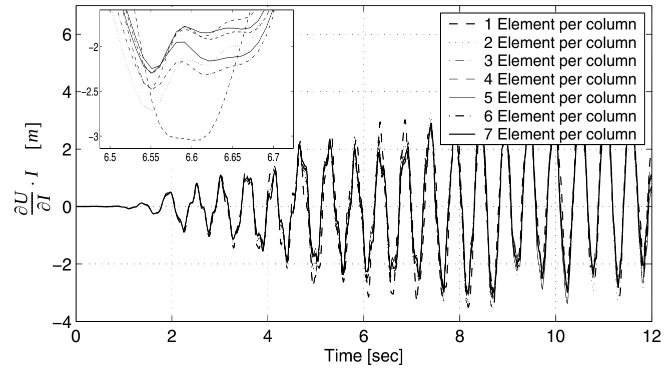

Figure 15. Sensitivity of roof displ. to I with increasing number of finite elements per beam/ column.

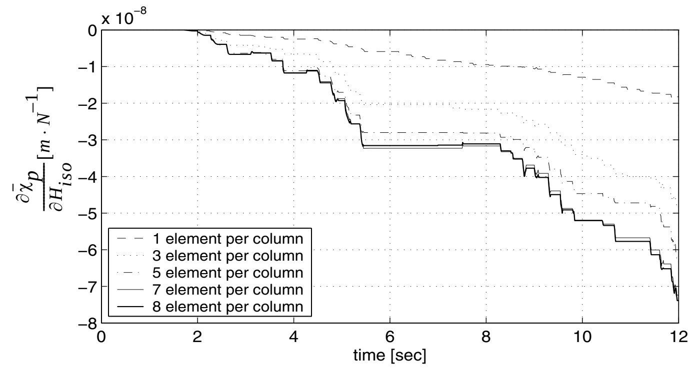

Figure 16. Sensitivity of $\bar{\chi}_p$ to H_{iso} with increasing number of finite elements per beam/column.

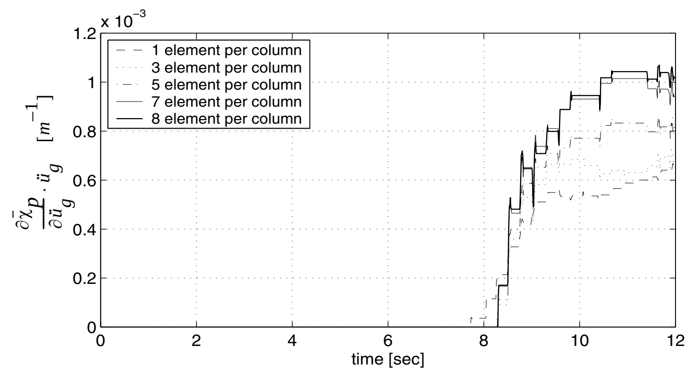

Figure 17. Sensitivity of $\bar{\chi}_p$ to $\ddot{u}_g(t = 7.60\ sec)$ with increasing number of elements per beam/column.

Table 3: Minimum number of elements per beam/ column required for convergence of local responses and their sensitivities.

	$M-\chi$	χ_p	$\frac{\partial \chi_p}{\partial I}$	$\frac{\partial \chi_p}{\partial M_{y0}}$	$\frac{\partial \chi_p}{\partial H_{iso}}$	$\frac{\partial \chi_p}{\partial H_{kin}}$	$\frac{\partial \chi_p}{\partial \ddot{u}_g(7.60 sec)}$
Static		5	6	6	6	6	
Dynamic	3	5	7	7	7	7	7

	$\bar{\chi}_p$	$\frac{\partial\bar{\chi}_p}{\partial I}$	$\frac{\partial\bar{\chi}_p}{\partial M_{y0}}$	$\frac{\partial\bar{\chi}_p}{\partial H_{iso}}$	$\frac{\partial\bar{\chi}_p}{\partial H_{kin}}$	$\frac{\partial\bar{\chi}_p}{\partial \ddot{u}_g(7.60sec)}$
Static	5	6	6	6	6	
Dynamic	5	7	7	7	7	7

3 elements per beam/column. The time step size is varied from 0.02 sec to 0.0005 sec. Some computational results are shown in Figs. 18 to 22. Furthermore, for each response parameter and load case, the maximum time step size required to achieve convergence of response and response sensitivities is reported in Table 4 for the global response parameter U and in Table 5 for the local response parameters.

Based on the single application example and the small set of response parameters considered in this study, it is observed that:

(1) The global response parameter converges at a time step size larger than or equal to that required for convergence of local response parameters.
(2) Both global and local response parameters converge at a time step size larger than or equal to that required for convergence of the corresponding sensitivities.
(3) Sensitivities of global and local response parameters tend to converge at the same time step size.

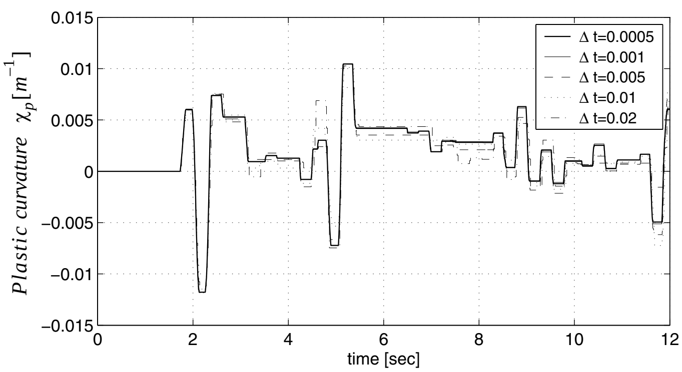

Figure 18. Convergence of plastic curvature χ_p with respect to time step size.

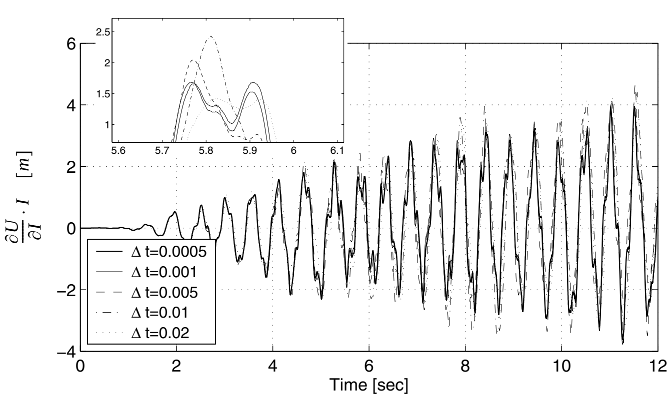

Figure 19. Convergence of roof displacement sensitivity to I with respect to time step size.

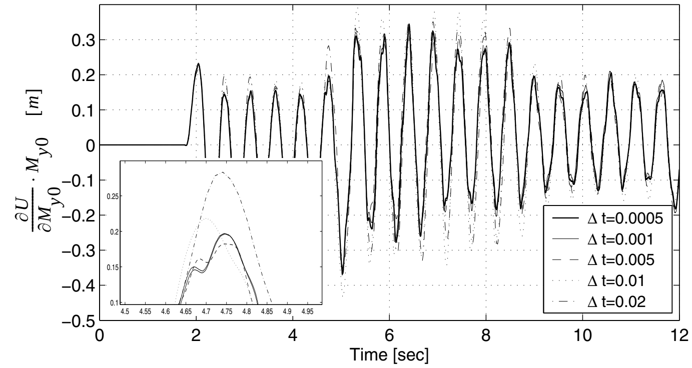

Figure 20. Convergence of roof displacement sensitivity to M_{y0} with respect to time step size.

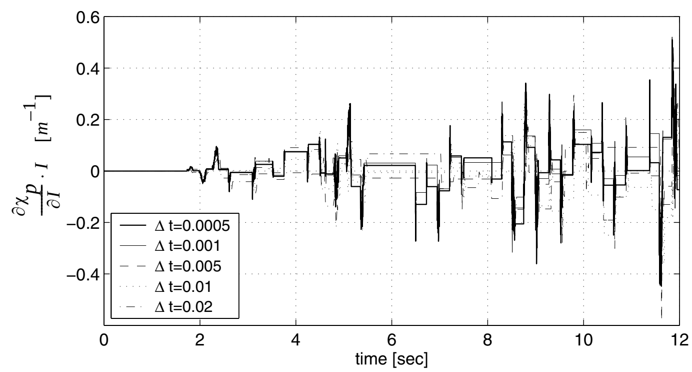

Figure 21. Convergence of plastic curvature sensitivity to I with respect to time step size.

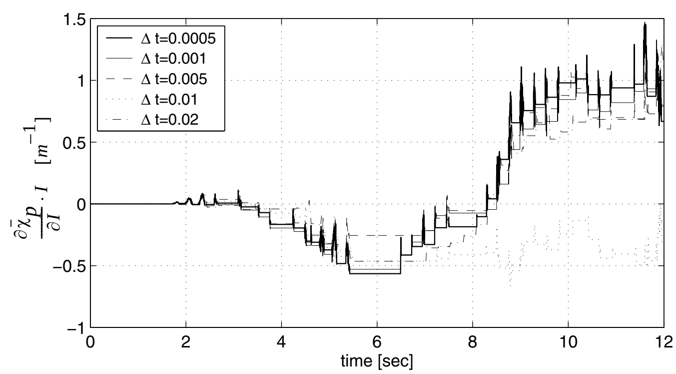

Figure 22. Convergence of accumulated plastic curvature sensitivity to I with respect to time step size.

Table 4: Maximum time step size required for convergence of global response and its sensitivities.

$\frac{\partial U}{\partial I}$	$\frac{\partial U}{\partial M_{y0}}$	$\frac{\partial U}{\partial H_{iso}}$	$\frac{\partial U}{\partial H_{kin}}$	U
10^{-3}	10^{-3}	10^{-3}	10^{-3}	5×10^{-3}

Table 5: Maximum time step size required for convergence of local responses and their sensitivities.

$M-\chi$	χ_p	$\frac{\partial\chi_p}{\partial I}$	$\frac{\partial\chi_p}{\partial M_{y0}}$	$\frac{\partial\chi_p}{\partial H_{iso}}$	$\frac{\partial\chi_p}{\partial H_{kin}}$	$\frac{\partial\chi_p}{\partial \ddot{u}_g(7.60sec)}$
5×10^{-3}	10^{-3}	10^{-3}	10^{-3}	10^{-3}	10^{-3}	10^{-3}

$\bar{\chi}_p$	$\frac{\partial\bar{\chi}_p}{\partial I}$	$\frac{\partial\bar{\chi}_p}{\partial M_{y0}}$	$\frac{\partial\bar{\chi}_p}{\partial H_{iso}}$	$\frac{\partial\bar{\chi}_p}{\partial H_{kin}}$
10^{-3}	10^{-3}	10^{-3}	10^{-3}	10^{-3}

4 CONCLUSIONS

The Direct Differentiation Method (DDM) allows to compute the "exact" sensitivities of the numerical nonlinear finite element response prediction of a structural system to material and loading parameters. Three types of convergence studies related to the DDM were performed, namely (1) convergence of the sensitivity results obtained using the forward finite difference method towards those obtained using the DDM, with decreasing relative size of the sensitivity parameter increment, $\Delta\theta/\theta$; (2) convergence of response and response sensitivities with respect to spatial discretization (i.e., finite element mesh size); and (3) convergence of response and response sensitivities with respect to temporal discretization (i.e., time step size). These sensitivity studies were conducted based on a test structure consisting of a steel moment-resisting frame subjected to monotonic push-over and earthquake base excitation. The frame is modeled using a simple 2-D displacement-based, plasticity-based (1-D J_2 plasticity) frame element. Based on the results obtained for this inelastic test structure, it was found that:

(1) For each loading case and each sensitivity parameter θ, there is an optimum value of $\Delta\theta/\theta$ for which the finite difference results are closest to the DDM results. Above or below this optimum value, the finite difference results are worsened by truncation error or condition error, respectively.

(2) A given response parameter, global or local, converges with fewer elements per beam/column than its sensitivities.

(3) Global and local response parameters converge at a time step size larger than or equal to that required for convergence of the corresponding sensitivities.

This study shows that the spatial and temporal (to a lower degree) discretization requirements for accurate computation of the structural response are different from those for accurate computation of the response sensitivities to material and loading parameters. In the application example considered, the spatial discretization requirements for accurate computation of the response sensitivities also depend on the sensitivity variable.

5 ACKNOWLEDGEMENTS

Support for this research by the Pacific Earthquake Engineering Research (PEER) Center through the Earthquake Engineering Research Centers Program of the National Science Foundation under Award number EEC-9701568 is gratefully acknowledged.

REFERENCES

Chopra, A.K. 2001. *Dynamics of Structures: Theory and Applications to Earthquake Engineering*. Second Edition, Prentice Hall.

Conte, J. P. & Jagannath, M. K. 1995a. Seismic Reliability Analysis of Concrete Gravity Dams. *A Report on Research Sponsored by the Main Italian Electricity Company (ENEL)*, Department of Civil Engineering, Rice University, Houston, Texas, April 1995.

Conte, J.P., Jagannath, M.K. & Meghella, M. 1995b. Earthquake response sensitivity analysis of concrete gravity dams. *Proc. Seventh International Conference on Applications of Statistics and Probability*, Paris, France, July 10-13, 1995b: 395-402.

Conte, J.P. & Vijalapura, P.K. 1998. Seismic Safety Analysis of Concrete Gravity Dams Accounting for Both System Uncertainty and Excitation Stochasticity. *A Report on Research Sponsored by the Italian National Power Board (ENEL-CRIS)*, Department of Civil Engineering, Rice University, Houston, Texas, June 1998.

Conte, J.P. & Vijalapura, P.K. 2000. Time-variant reliability analysis of hysteretic SDOF systems with uncertain parameters and subjected to stochastic loading. *Proc. Eighth International Conference on Applications of Statistics and Probability*, Sydney, Australia, 12-15 December, 1999: 827-834.

Conte, J. P. 2001. Finite element response sensitivity analysis in earthquake engineering. *Earthquake Engineering Frontiers in the New Millennium*, Spencer & Hu (Eds), Swets & Zeitlinger, 2001: 395-401.

Conte, J.P., Vijalapura, P.K. & Meghella, M. 2002. Consistent finite element response sensitivities in seismic reliability analysis. *J. of Engrg. Mech.*, ASCE, accepted for publication.

Kleiber, M., Antunez, H., Hien, T.D. & Kowalczyk, P. 1997. *Parameter Sensitivity in Nonlinear Mechanics: Theory and Finite Element Computations*. Wiley.

Li, C.-C. & Der Kiureghian, A. 1995. Mean out-crossing rate of nonlinear response to stochastic input. *Proc. Seventh International Conference on Applications of Statistics and Probability*, Paris, France, July 10-13, 1995: 295-302.

Liu, P. L., and Der Kiureghian, A. 1991. Finite element reliability of geometrically nonlinear uncertain structures. *Journal of Engineering Mechanics*, ASCE, Vol. 117(EM8): 1806-1825.

Simo, J.C. & Hughes, T.J.R. 1998. *Computational Inelasticity*. Springer-Verlag.

Taylor, R.L. 1998. FEAP - A Finite Element Analysis Program - Version 7.1 User Manual. Department of Civil and Environmental Engrg., Univ. of California at Berkeley, Berkeley, CA, 94720-1710, November, 1998 (http://www.ce.berkeley.edu/~rlt/feap/).

Zhang, Y. & Der Kiureghian, A. 1993. Dynamic Response Sensitivity of Inelastic Structures. *Comp. Methods Appl. Mech. Eng.*, 108: 23-36.